

WADC TECHNICAL REPORT 57-267

ASTIA DOCUMENT NO. AD 130967

INCOMPRESSIBLE POTENTIAL FLOW PREDICTION
FOR AXIALLY SYMMETRIC DUCTED BODIES

**INCOMPRESSIBLE POTENTIAL FLOW PREDICTION
FOR AXIALLY SYMMETRIC DUCTED BODIES**

PHILIP LAVINE

AERONAUTICAL RESEARCH LABORATORY

AUGUST 1957

**Project 3666
Task 70151**

**WRIGHT AIR DEVELOPMENT CENTER
AIR RESEARCH AND DEVELOPMENT COMMAND
UNITED STATES AIR FORCE
WRIGHT-PATTERSON AIR FORCE BASE, OHIO**

Approved for public release by AFM, G.
FBI - October 1972

100000

This report was prepared for the Fluid Dynamics Research Project
of the National Advisory Committee on Research, Wright-Patterson Air Force Base, Ohio.
Project 7000, Aeromechanics Division, Wright-Patterson Air Force Base.

The author gratefully wishes to acknowledge Professor A. M. Barnard
of Ohio State University, for his helpful guidance, Dr. G. C. Candler,
Chief of the Mathematics Group at NACA, for stimulating discussions,
and to the members of the Numerical Aerodynamics Group, especially
Dr. J. Mizell and Lt. Brown for their tremendous effort in preparing

ABSTRACT

The velocity potentials and stream functions for a point source, doublet, and source, sink, dipole, and doublet in a semi-infinite wedge and line sources are derived for the case of axially symmetric incompressible potential flow in an infinitely long duct of constant diameter.

Methods for the development of arbitrary body shapes in uniform sheet flow are presented. Several practical applications are indicated.

PUBLICATION REVIEW

THIS REPORT HAS BEEN REVIEWED AND IS APPROVED.

FOR THE COMMANDER:

Merton J. Traxler
Merton J. Traxler
Colonel, USAF
Chief, Aerometrical Research Laboratory
Directorate of Laboratories

TABLE OF CONTENTS

INTRODUCTION	1
ANALYSIS	2
1. Point Sources in the Free Field	3
2. Doublet in the Free Field	7
3. Line Sources	9
4. Ring Doublets	10
5. Disk Sources	10
6. Disk Doublets	11
7. Ring Vortex	12
8. Line Sources	12
APPLICATIONS	
A. Simple Bodies	13
1. Point Source in a Uniform Flow	13
2. Rankine in a Uniform Flow	15
3. Ring Doublet in a Uniform Flow	15
4. Disk Doublet in a Uniform Flow	16
B. Prescribed Body Shape	16
1. Discrete Distributions of Sources and Sinks	16
2. Discrete Distributions of Sources and Sink Dipoles	19
C. Precessing and Joggling Concentric and Parabolic Distributions	19
1. Precessing Concentric Distributions	19
2. Joggling Concentric Distributions	19
D. Influence of Local Obstacles	20
CONCLUDING REMARKS	20
TABLES I - III	21-22
APPENDICES I - III	23-24
REFERENCES	25-26
FIGURES 1-12	27-28

NOTATION

- a radius of a ring or disk source, sink or sinklet.
- e natural logarithm base; $e = 2.71828$
- r stream function
- \tilde{X}_1, \tilde{X}_2 modified Bessel functions of the first and second kind respectively
- λ eigenvalue
- $\tilde{\Psi}, \tilde{\Upsilon}$ stream function of the first and second kind respectively.
- Q strength of a source or sink form
- N strength of a sinklet form
- r' dimensionless radial coordinate; ratio of radial distance to dust radius.
- s ratio of $2\pi/\theta$
- U superimposed uniform flow velocity
- z dimensionless axial coordinate; ratio of axial distance to dust radius
- ϕ velocity potential
- \tilde{U}_1, \tilde{U}_2 axial and radial velocity components respectively
- $\tilde{\Lambda}$ constant value sign

$r' = 171/2a$

$\tilde{U}_1 = 16.15/2a$

$\tilde{U}_2 = 8.7/2a$

Abbreviations:

- * partial differentiation with respect to (z)
- ** partial differentiation with respect to (z^2)
- $n, n+1$ consecutive numbers; i.e. 2, 3, 4, 5, . . .

INTRODUCTION

The problem of determining the complete flow field about axially symmetric bodies occurs widely. Typical instances are the design and analysis of the performance of axisymmetric nose cone and fairings retaining sonic booms, configurations used in wind tunnel test arrangements, ring type flame holders, and turbulent boundary layers generally. In view of the numerous practical applications, it was deemed to initiate a study of the problem for the case of incompressible flow.

Little theoretical work has been published concerning the flow about ducted axisymmetric bodies, especially for the case where the body fills a sizable portion of the cross sectional area of the duct. The present theoretical study was well advanced before it was discovered that a solution for a point source in an infinitely long duct of constant diameter had recently been published (Ref. 1). A numerical error occurs, however, in the expression for the velocity potential of a source as given there. The expression is redefined here, as it forms the basis for the development of a general approach to the study of the flow past ducted axisymmetric bodies.

*This manuscript was submitted by the author on application on October 1954.

In addition to be considered in the case of steady, incompressible and potential flow about axisymmetric bodies, control on the value of ∞ indefinitely large, allowing this of constant flow over the outer boundary system and the inner boundary system shown in Fig. 1.

The differential equation for the velocity potential of an axisymmetric incompressible flow is well known, and may be written as (Ref. 2),

$$\nabla^2 \phi + \frac{1}{r} \frac{\partial \phi}{\partial r} + \Phi_{\infty} = 0 \quad (1)$$

Fortunately, this equation is amenable to separation by the method of separation of variables. Further, Equation 1 is linear, so that the principle of superposition can be utilized to build up complex solutions by merely adding simple solutions together.

1. Point Source on the Radial Axis

An expression for the velocity potential of a point source will be developed first. Once it is in hand, the potential solutions for a sink and a doublet follow directly. These solutions may be superimposed on each other to construct axisymmetric bodies of the desired shape.

Consider a source, of strength (m), as shown in Fig. 2, located at $r = 0$. The boundary conditions which must be satisfied are:

I. The source flow is uniform at $r = 1 \text{ cm}$. Thus,

$$(\phi_s)_{r=1 \text{ cm}} = 0$$

II. At $r = \infty$, the velocity of the source ((m)), and at $r = \infty$, the velocity of the source flow is $(-\infty)$. This follows from continuity as the total source flow exists in both about the (r) axis. The (-1) sign accounts for the velocity direction as indicated in Fig. 1.

III. The radial component of the velocity is zero at the first wall. Thus,

$$(\dot{v}_r)_{r=0} = 0$$

IV. The source flow is symmetric about the (r) axis as well as the (s) axis. However, a singularity exists at $r = 0$. Hence, $(\dot{v}_r)_{r=0} = 0$ for $r \neq 0$. Proceeding by the method of separation of variables, let

$$R = R_1 J_0(x) \quad (2)$$

and substituting into Eq. 1, yields

$$\frac{1}{x} R_{11} + \frac{1}{x^2} R_1 = - \frac{1}{x^2} f_{11} \quad (3)$$

Since (1) and (2) are independent, the only possible solutions to Eq. 1 is

$$\frac{1}{x} R_{11} + \frac{1}{x^2} R_1 = - \frac{1}{x^2} f_{11} = k = \text{constant} \quad (4)$$

From which three possibilities: $x = 0$, $x = j^2$, $x = -j^2$, where j^2 is a constant.

Examining the case of $x = j^2$, $j \neq 0$, one finds

$$R_{11} = j^2 = 0$$

$$R_{11} + \frac{1}{x} R_1 + j^2 R = 0$$

The solutions to the above equations are well known, as

$$R_1 = C_1 e^{-jx} + C_2 e^{jx}$$

and

$$R = C_1 J_0(jx) + C_2 Y_0(jx)$$

respectively, where (J_0) is the Bessel function of the first kind of zero order, and (Y_0) is the Bessel function of the second kind of zero order. Therefore, a solution to Eq. 1 exists in the form

$$S = (D_1 e^{-jx} + D_2 e^{jx}) (C_1 J_0(jx) + C_2 Y_0(jx))$$

To satisfy conditions I and II, it is apparent that $D_1 = 0$ and either $D_2 = 0$ or $C_1 = 0$. Assuming the former, since jx is positive or negative, hence, one can write,

Further, to satisfy condition III, the solution must have the form,

$$S = A e^{-jx} + B e^{jx} J_0(jx)$$

where the term (λ_m) can be thought as an equivalent to λ_0 . In the case of $k = 0$.

The condition III, requires that

$$\lambda_1(j) = 0$$

Therefore, the values of (j) are the nth-order roots of (J_1) , where (J_1) is the Bessel function of the first kind of first order. The form of the solution then becomes,

$$A_0 = 2\pi m + A_0 e^{-im\theta} J_0(\frac{1}{m}r) \quad (5)$$

There is now a solution corresponding to each value of (j) . It should be noted that conditions I, II and III have been satisfied. To satisfy condition IV, a series solution can be built up, using Eq. 5, whereby,

$$S = 2\pi m + \sum_{n=1}^{\infty} A_n e^{-in\theta} J_n(\frac{1}{m}r)$$

Introducing condition IV into Eq. 6, one has,

$$(A_n)_{nm} = 2\pi m - \sum_{n=1}^{\infty} A_n J_n(\frac{1}{m}r)$$

The orthogonality property of Bessel functions is such that (Ref. 3)

$$\int_0^1 r J_n(\frac{1}{m}r) J_m(\frac{1}{m}r) dr = \begin{cases} 0 & n \neq m \\ \frac{2}{m} & n = m \end{cases}$$

Using the above property, we obtain

$$\int_0^1 r J_n(\frac{1}{m}r) (A_n)_{nm} dr = 2\pi \int_0^1 r J_n(\frac{1}{m}r) dr = A_n \frac{1}{m} \int_0^1 r J_0^2(\frac{1}{m}r) dr$$

The second integral on the right can be readily evaluated (Ref. 3) and

$$A_n \frac{1}{m} \int_0^1 r J_0^2(\frac{1}{m}r) dr = \frac{1}{2} \pi m^2 J_0^2(\frac{1}{m})$$

the first integral on the right is zero, as

$$\int_0^1 J_0(1_{\infty} r) dr = \frac{1}{2} \left[J_1(1_{\infty}) \right]_0^1 = 0$$

Thus,

$$A_0 = \frac{-2}{4J_0^2(1_{\infty})} \int_0^1 (A_0)_{\text{max}} J_0(1_{\infty} r) dr$$

Taking the size of the source to be very small (down to a mathematical point), one can write, in accordance with Condition IV,

$$A_0 = \frac{-2}{4J_0^2(1_{\infty})} \lim_{r \rightarrow 0} \int_0^r (A_0)_{\text{max}} J_0(1_{\infty} r) dr$$

But, $\lim_{r \rightarrow 0} J_0(1_{\infty} r) = 1$, so that one has,

$$A_0 = \frac{-2}{4J_0^2(1_{\infty})} \cdot \frac{1}{2\pi} \lim_{r \rightarrow 0} \int_0^{2\pi} \int_0^1 (A_0)_{\text{max}} dr d\theta$$

The integral above represents the P/CW emitted by the source, which is $(2\pi n)$ in either direction by Gauss's theorem, so that

$$A_0 = \frac{-2n}{4J_0^2(1_{\infty})}$$

A solution to Eq. 1, satisfying the four boundary conditions can now be obtained by substituting the equation for the coefficients (A_m) into Eq. 6, yielding,

$$\phi = 2\pi m + m \sum_{n=1}^{\infty} \frac{e^{inx}}{4J_0^2(1_{\infty})} J_0(1_{\infty} r) \quad (7)$$

Returning to Eq. 4, and examining the case of $\lambda = j_0^2$, one finds that the boundary conditions cannot be satisfied with a series type of solution. Details of this case are presented in Appendix I.

The stream function corresponding to the above velocity potential is

$$\bar{F} = \pm\pi r^2 \mp 2\pi r \sum_{n=1}^{\infty} \frac{-i_n l n l}{j_n J_0^2(j_n)} J_1(j_n r) \quad (8)$$

sign convention: (+) for $z > 0$
(-) for $z < 0$

At $z = 0$, the stream function is discontinuous, so that approaching $z = 0$ from the left (see Fig. 2), $\bar{F} = -\infty$, while approaching $z = 0$ from the right, $\bar{F} = +\infty$.

That Eq. 8 represents the stream function may be seen by direct substitution into the following relationships for axisymmetric, incompressible, potential flow,

$$\frac{d\bar{F}}{dr} = -\frac{1}{r} F_r \quad \frac{d^2\bar{F}}{dr^2} = \frac{1}{r^2} F_{rr} \quad (9)$$

The solution for a sink follows directly, as it influences the derived velocity potential and stream function only through the sign (?) associated with the strength (m).

The axial and radial velocity components can be determined by the appropriate partial differentiation of Eq. 7, so that,

$$F_r = \pm 2\pi \mp 2\pi \sum_{n=1}^{\infty} \frac{-i_n l n l}{J_0^2(j_n)} J_0(j_n r) \quad (10)$$

sign conventions: (+) for $z > 0$
(-) for $z < 0$

$$\bar{F}_r = 0 \quad \text{at } z = 0$$

$$\frac{F_r}{r} = 2\pi \sum_{n=1}^{\infty} \frac{-i_n l n l}{J_0^2(j_n)} J_1(j_n r) \quad (11)$$

To calculate the streamlines and velocity components, it is convenient to introduce,

$$r^2 = \frac{M^2}{\pi}, \quad f_1' = \frac{1}{2\pi} \ln \frac{r}{R}, \quad f_2' = -\frac{1}{2\pi} \ln \frac{r}{R}$$

Fortunately, the values of $J_0(jr)$ and $J_1(jr)$ over the range $r = 0(.02)1$ have been tabulated in Reference 5; for the first ten roots of J_1 . After the first ten roots have been used, the difference in the roots is close enough to $\pi/2$ so that additional terms can be rapidly evaluated by using the asymptotic approximation given in References 5 and 6.

$$J_n(V) \xrightarrow[V \rightarrow \infty]{} (2/\pi V)^{1/2} \cos(V - n\pi/2 - \pi/4) \quad (12)$$

For values of $V > 15$, the above relationship is in agreement with the exact value to within one percent, (ref. 7). For larger values of V , the approximation becomes more accurate. Values of T^2 , T_1 , T_2 were calculated on a Remington Rand 1103 computer at the Aerautical Research Laboratory of the Wright Air Development Center. The results are presented in Tables I, II, III. Sufficient values are included in these tables to facilitate the analysis of flow about bodies of arbitrary shape.

The asymptotic relationship was used to calculate enough terms to assure convergence to five decimal places for the values of α_j for $j \leq 1$, $s = .1$, and $s = .2$. The remaining values are tabulated for the first ten roots of J_1 only. For $s \neq \alpha_j$, the first ten roots were sufficient to obtain convergence to five decimal places. For values of $s \neq 1$, only one or two terms are necessary, hence the tables were restricted to values of $s \leq 1$. Scientific notation is used throughout the tables, so that the number and sign preceding the tabulated values locate the decimal place. For example, $.746552$ may be written as $.074655$.

For a point source not located at the origin, one has only to consider that (z) (in Eqs. 8, 10, 11) represents the distance along the (z) axis from the plane of the source to the point where the velocity or stream function is being evaluated. In this regard, the absolute value signs (|z|) were dropped throughout the tables for convenience.

2. Doublet on the Tube Axis

To derive the velocity potential for a doublet, one can consider a sink at the origin and a source of the same strength at $z = A z$, $r = 0$, as shown in Fig. 3. The expressions for the source and sink follow from the development above.

$$\phi_{so} = 2m(z - az) - 2m \sum_{n=1}^{\infty} \frac{-i_n(z - az)}{i_n J_0'(i_n)} J_0(i_n r)$$

$$\phi_{si} = 2mz + 2m \sum_{n=1}^{\infty} \frac{i_n(z)}{i_n J_0'(i_n)} J_0(i_n r)$$

At the point (r), the velocity potential due to the source and sink, taken as the limit as $az \rightarrow 0$, is

$$\lim_{az \rightarrow 0} (\phi_{so} + \phi_{si}) = \lim_{az \rightarrow 0} 2m \sum_{n=1}^{\infty} \frac{-i_n z}{i_n J_0'(i_n)} J_0(i_n r) (1 - e^{-i_n az}) = 2mz$$

or, expanding,

$$\lim_{az \rightarrow 0} 2m \sum_{n=1}^{\infty} \frac{-i_n z}{i_n J_0'(i_n)} J_0(i_n r) (-i_n ar - \frac{(i_n az)^2}{2} - \frac{(i_n az)^3}{3} - \dots) = 2mz$$

The strength of the doublet is defined as,

$$M = \lim_{az \rightarrow 0} 2mz$$

Thus, only the first term remains in the expansion above, so that the velocity potential for a doublet located at the origin is;

$$\phi = -M \sum_{n=1}^{\infty} \frac{-i_n i_m}{J_0'(i_n)} J_0(i_n r) = Mz \quad (13)$$

$$\psi = 2M \sum_{n=1}^{\infty} \frac{-i_n i_m}{J_0'(i_n)} J_1(i_n r) \quad (14)$$

One should note the sign convention adopted above for the doublet, for as derived, the axis of the doublet lies on the (z) axis and the doublet flow is counter clockwise above the (z) axis.

The streamlines for a doublet are shown in Figure A. The calculations for the doublet were carried out in much the same manner as the case for the source streamlines. However, Eq. 14 converges much more slowly than does Eq. 8, requiring a greater number of terms.

In addition, the limit of Eq. 6 is known, at $s = 0$, by symmetry and continuity, to be $V = m$, but at $s = \infty$, A_0 is more difficult to evaluate. From the nature of the doublet, however, the slopes of the streamlines must be zero at $s = 0$, hence, A_0 is evaluated for values of (x) close to zero, and then the streamlines were fared in. To estimate the value of A_0 , at $s = 0$, slopes of the curves corresponding to Eqs. 6 and 7 were found graphically at $s = 0$.

3. Ring Source.

The velocity potential of a ring source can be found using the same line of attack as used for the single source. The boundary conditions put forth for the point source are valid in this case also, except for condition IV, which must be modified as follows:

IV(a) The source flow is symmetric about the (r) axis. However, the ring $r = a$ is a singularity. Thus,

$$(A_2)_{\text{ring}} = 0 \text{ for } r \neq a$$

The total strength of the ring, which is taken to be uniformly distributed around the circumference, is (m) , so that the total source flow emitted by the ring is $(4\pi m)$. Therefore, Eqs. 6-10 are valid for a ring source as well as a point source. To obtain the coefficients (A_n) , the condition must be satisfied that,

$$A_0 = \frac{\pi^2}{4m^2 C(A_0)} \lim_{\epsilon \rightarrow 0} \int_{-\infty}^{+\infty} (A_2)_{\text{ring}} J_0(j_m r) dr$$

But this may be written as,

$$A_0 = \frac{\pi^2}{4m^2 C(A_0)} J_0(\frac{j_m a}{2}) \frac{1}{2\pi} \int_{-a}^{+a} (A_2)_{\text{ring}}^2 dr$$

The integral now represents the flow emitted by the ring source, which is $(2\pi m)$ in either direction, so that,

$$A_0 = \frac{\pi^2}{4m^2 C(A_0)} J_0(\frac{j_m a}{2})$$

The velocity potential for the ring source follows,

$$V + iB_{\text{ring}} = \frac{m}{2\pi} \sum_{n=1}^{\infty} \frac{(-1)^n j_n}{4m^2 C(A_0)} J_0(\frac{j_n a}{2}) J_0(\frac{j_n r}{2}) \quad (15)$$

The corresponding stream function, satisfying Eq. 7, is

$$\Psi = \frac{U_0 r^2}{2} + 2\pi \sum_{n=1}^{\infty} \frac{-i A_n j_n l_n}{J_0^2(l_n)} J_1(l_n r) J_0(l_n a) \quad (16)$$

sign convention: $\begin{cases} (+) \text{ for } a > 0 \\ (-) \text{ for } a < 0 \end{cases}$

At $a = 0$, $J_0(l_n a) \rightarrow 1$, depending on whether the plane of the ring source is approached from the right or left.

A check on the validity of the solution can be made by taking the limit as ($a \rightarrow 0$) so that ($J_0(l_n a) \rightarrow 1$) and the expressions reduce to those found for a point source on the axis.

4. Ring Doublet

The velocity potential for a ring doublet and the corresponding stream function can be obtained by using the same techniques as used to obtain the point doublet. The resultant expressions are,

$$\phi = -2V - 2\pi \sum_{n=1}^{\infty} \frac{-i A_n l_n}{J_0^2(l_n)} J_0(l_n r) J_0(l_n a) \quad (17)$$

$$\Psi = 2\pi \sum_{n=1}^{\infty} \frac{-i A_n l_n}{J_0^2(l_n)} J_1(l_n r) J_0(l_n a) \quad (18)$$

5. Disk Source

The velocity potential of a disk source can be derived using the same boundary conditions as for the case of the point source, except condition IV, which must be modified as,

IV(b) The source flow is symmetrical about the (r) axis. However, the disk of radius $r = a$ is a singularity. Thus,

$$(\phi_s)_{r=a} = 0 \text{ for } r > a$$

The total strength of the doublet, which is taken to be uniformly distributed over the disk, is (A_0). Returning to Eq. 6, the coefficients (A_n) can be determined by utilizing condition IV(b), such that,

$$A_0 = \frac{-2}{\pi J_0^2(l_n)} \int_0^1 (E_n)_{r=a} J_0(l_n r) r dr$$

by continuity, $\phi^*(\theta_1)_{|z=0} = \infty$, so that,

$$A_n = \frac{-2}{4J_0^2(j_n)} \quad \frac{2a}{a^2} \int_0^a J_0(j_n x) dx$$

or,

$$A_n = \frac{-2a}{a^2 J_0^2(j_n)} J_1(j_n a)$$

The expression for the velocity potential follows,

$$\phi = \pm 2m - 2a \sum_{n=1}^{\infty} \frac{-j_n j_{n-1}}{a^2 J_0^2(j_n)} J_0(j_n x) J_1(j_n a) \quad (29)$$

$$\psi = \pm m^2 \pm 4m \sum_{n=1}^{\infty} \frac{-j_n j_{n-1}}{a^2 J_0^2(j_n)} J_1(j_n x) J_1(j_n a) \quad (20)$$

sign convention: (+) for $a > 0$
(-) for $a < 0$

At $x = 0$, $\psi = \infty$, depending on whether the plane of the disk source is approached from the right or left. The results can be checked by taking the limit as ($a \rightarrow 0$), whereupon $J_0(j_n a) \rightarrow j_n a$, so that the above expressions reduce to those for a point source.

Comparing Eqs. 20 and 6, it is apparent that the convergence of Eq. 20 will be faster, so that the use of disks for developing better or general shapes rather than point sources should reduce the amount of computation.

6. Disk Doublet

The velocity potential for a disk doublet can be found by utilizing the techniques used for a point doublet. The velocity potential is found to be,

$$\phi = -2m - 2a \sum_{n=1}^{\infty} \frac{-j_n j_{n-1}}{a^2 J_0^2(j_n)} J_0(j_n x) J_1(j_n a) \quad (21)$$

The corresponding stream function is:

$$\psi = 4\pi k \sum_{n=1}^{\infty} \frac{a_n l_{n1}}{j_n J_0^2(j_n)} J_1(j_n r) J_1(j_n a) \quad (22)$$

7. Ring Vortex

The velocity potential for a ring vortex is readily obtained by employing the property that a ring vortex is equivalent to a uniform distribution of doublets over the surface bounded by it. (ref. 2). The axes of the doublets are taken normal to the surface everywhere, and the density of the distribution is taken to be equal to the strength of the vortex. Thus, by Eq. 21, one has,

$$\phi = -2\pi a^2 K - 4\pi k \sum_{n=1}^{\infty} \frac{a_n l_{n1}}{j_n J_0^2(j_n)} J_0(j_n r) J_1(j_n a) \quad (23)$$

where (K) is the strength of the vortex.

The corresponding stream function is:

$$\psi = 4\pi a k r \sum_{n=1}^{\infty} \frac{a_n l_{n1}}{j_n J_0^2(j_n)} J_1(j_n r) J_1(j_n a) \quad (24)$$

8. Line Source

Continuous distributions of sources, sinks and doublets are often used to develop bodies of various shapes. Considering the case of a line source of constant strength per unit length (m_1), and letting (x_1) be the source coordinate, then,

$$d\phi = 2m_1(x-x_1)dx_1 - 2m_1 \sum_{n=1}^{\infty} \frac{a_n l_{n1}(x-x_1)}{j_n J_0^2(j_n)} J_0(j_n r) dx_1$$

so that the velocity potential is,

$$\phi = 2m_1 - m_1(x_0+x_p) - \frac{2m_1}{\pi j_0} \sum_{n=1}^{\infty} \frac{a_n l_{n1} e^{-j_n x_0}}{j_n J_0^2(j_n)} J_0(j_n r) (e^{j_n x_p}) \quad (25)$$

where (x_0) and (x_p) denote the beginning and end of the source respectively, and (x_p) is the length of the source. The corresponding stream function is,

$$P = \frac{U_0^2}{\pi} - \frac{2\pi}{3} \sum_{n=1}^{\infty} \frac{-i_n \ln a_n l}{\frac{1}{2} r^2 (1_n)} J_1(i_n r) (e^{i_n \theta_n l}) \quad (26)$$

The results can be checked by taking the limit as $a_n \rightarrow 0$ whereupon the expressions reduce to those for a point source. The convergence of the functions above does not appear to be any better than for the case of a point source, so that the additional complexity of the results may not warrant the use of continuous distributions. Linear or exponential variations of the source strength can be treated in the same manner as the above case, but the resultant expressions become increasingly cumbersome.

TYPICAL APPLICATIONS

A. SIMPLE BODIES

The study of bodies of arbitrary and practical shape will be initiated by first considering the simple shapes resulting when single sources, infinite, disk doublets and ring doublets of varying strength are placed in a ducted uniform flow.

1. Point Source in a Uniform Flow

The velocity potential of a point source in a ducted uniform flow is found by adding the velocity potential (U_0) for a uniform flow to Eq. 7. To obtain the corresponding stream function, one has to add the term ($Ur^2/2$) to Eq. 8. In addition, a constant ($2m$) must be subtracted from the stream function since the flow downstream of the source is being considered.

The form of the stream function indicated above stems from the mechanism by which a body streamline is developed when a point source is placed in a uniform flow. The source flow going upstream is turned back by the superimposed flow, so that upstream of the source, there is no net source flow (in the (z) direction) within the body streamlines. However, downstream of the source, both the original downstream source flow and the original upstream source flow which has been turned back downstream now exists (i.e., the total source flow). The usual convention for the stream function, is that a body streamline is indicated when its value is zero, i.e., $\psi = 0$. In order to retain this convention, it is then necessary to adjust the expression for the stream function downstream of the source by subtracting a constant which accounts for the source flow within the body streamlines. In this case, the constant is $(2m)$ as the stream function concerns only the flow in the upper half plane.

Tables were calculated for various source strengths using the results obtained from the analysis in the manner indicated above. To use the tables at the end of the text, the body streamline is determined by the condition that,

$$r^* = \frac{Ux^2}{\Delta u} \text{ for } z < 0$$

$$r^* = \frac{Ux^2}{\Delta u} + 1 \text{ for } z > 0$$

The results for several values of $(\Delta u/u)$ are shown in Fig. 5.

The radial components of the velocities, made dimensionless with (U) , are simply,

$$S_r = \frac{\Delta u}{U} S_0^*$$

which can be evaluated directly from Table III.

The axial velocity components can be evaluated similarly as,

$$S_z = (1 \pm 2\eta) S_0^*$$

sign convention: $\{+\}$ for $z > 0$
 $\{-\}$ for $z < 0$

At $z = 0$, $S_z = 0$. The axial velocity components can be evaluated by using Table II.

There is a departure from the usual result that the velocity upstream at infinity is just that due to the uniform flow superimposed on the source flow. In this case, the velocity upstream at infinity is less than the superimposed value by (Δu) . Similarly, the velocity downstream at infinity is greater by (Δu) .

The radius of the body at the plane of the source can be quickly found by employing the continuity equation, thus,

$$U - 2\eta = U(1 - r_0^2)$$

so that

$$r_0^2 = \frac{2\eta}{U}$$

The radius of the body downstream at $z = +\infty$ can also be determined by continuity as,

$$U(1 - \frac{r^2}{R^2}) = (U + 2w) (1 - \frac{r^2}{R^2})$$

It follows that,

$$\frac{r^2}{R^2} = 2 \frac{w}{U}$$

The formulae above indicate a criteria for the establishment of flow through the duct, namely, that ($U > 2w$). In order to establish the stagnation point, one can use Table II to determine at what value of (r),

$$(A_x')_{\text{true}} = \frac{U}{2w}$$

2. Doublet in a Uniform Flow

The velocity potential for a doublet in a uniform flow can be obtained by simply adding the velocity potential (U_0) for a uniform flow to Eq. 13. The corresponding stream function can be obtained by adding ($Ux^2/2$) to Eq. 14.

The body streamlines can be determined by using Table III, as the stream function can be written as,

$$\psi = \frac{U_0 r^2}{2} + 2w A_x'$$

Body calculated for several values of (M/U) are shown in Fig. 6. The calculation of the velocities was not attempted as the convergence close to the plume of the doublet is very poor.

3. Ring Doublet in a Uniform Flow

The velocity potential for a ring doublet in a uniform flow can be obtained by adding the velocity potential (U_0) for a uniform flow to Eq. 15. The corresponding stream function can be obtained by adding ($Ux^2/2$) to Eq. 16.

Care must be taken to observe the proper sign convention on (A_x), for to obtain a body, the doublet flow on the (x) axis and upstream of the doublet must be opposed to the direction of (U). Hence, if (U) is positive, (A_x) is negative.

A body calculated for $M/U = .5$ and $\epsilon = .5$, is shown in Fig. 7.

4. Point Doublet in a Uniform Flow

The velocity potential for a point doublet in a uniform flow can be obtained by adding the velocity potential (U_0) for a uniform flow to Eq. 21. The corresponding stream function can be obtained by adding $(Ur^2/2)$ to Eq. 22.

Results calculated for $(M = 40)$ and several values of (a) are shown in Fig. 8.

5. INFINITE BODY SHAPE

The velocity and pressure distributions about bodies of special shapes are often of practical interest. Numerous methods for the determination of the source and sink distribution corresponding to a non-ducted body occur in the literature (e.g., Ref. 8). Applying similar techniques to the case at hand, the author has developed a method for determining source and sink distributions which approximate a ducted body shape. Having the source and sink distribution is all that is required to completely define the velocity and pressure distribution about the body.

6. Discrete Distributions of Sources and Sinks

From the analysis of a point source in a uniform flow, it is clear that specifying one coordinate of the body surface determines the strength of the source (a). Consequently, for each specified body coordinate, one must place a source or sink in the flow. Since only axisymmetric bodies are being considered, the sources and sinks are located on the (z) axis. By judiciously choosing the location of these sources and sinks (i.e., close to the (z) coordinate specified or at least within the length of the desired body) one might expect that the body shape between the chosen coordinates will closely approximate the desired shape. To carry this approach out, it is convenient to let

$$r_s^2 = j_{\infty}^2 + \frac{z^2}{2} + r \sum_{n=1}^{\infty} \frac{\frac{a_n j_n z}{j_n J_0(j_n)}}{J_0(j_n)} J_1(j_n r) \quad (27)$$

Then the stream function for the total (s) sources in a uniform flow is,

$$\psi_t^* = \frac{r^2}{2} + \sum_{n=1}^s a_n \left(\frac{J_0(j_n r)}{j_n} \right) \quad (28)$$

where

$$j_n = \frac{\pi n}{L}$$

The sign associated with \bar{r}_z^0 sources has two possible meanings, respectively, namely (+) when $z > 0$, and (-) when $z < 0$, and at $z = 0$, $\bar{r}_z^0 = 1/2$, and the sign is negative. It was mentioned previously, but will be further emphasized here, that $|z|$ is the absolute value of the axial distance from the source in question to the point where the stream function or velocity potential is being evaluated. The value of $|z|$ is then relative to the source and not dependent on the arbitrary location of the origin of the coordinate system.

A previous analysis of the source flow inside the body streamlines indicated that the condition $\bar{r}_z^0 = 0$ defines a point on the body only if the net source flow upstream of this point (within the body) is zero. When a net source flow exists upstream of a particular point on the body, the condition

$$\bar{r}_z^0 = 1/2 \sum_{u=1}^n s_u$$

on the body, where (s_u) are the sources and sinks upstream of the body point.

As an example, consider that three body coordinates are specified, with sources and sinks located on the axis at the same values of (z) . Then, one has three equations,

$$\begin{aligned} 1/2\bar{r}_1^0 - S_1\bar{r}_{11}^0 - S_2\bar{r}_{21}^0 - S_3\bar{r}_{31}^0 &= 0 \\ 1/2\bar{r}_2^0 - S_1(1 - \bar{r}_{12}^0) - S_2\bar{r}_{22}^0 - S_3\bar{r}_{32}^0 &= 0 \\ 1/2\bar{r}_3^0 - S_1(1 - \bar{r}_{13}^0) - S_2(1 - \bar{r}_{23}^0) - S_3\bar{r}_{33}^0 &= 0 \end{aligned}$$

The subscripts are chosen to correspond to the coordinates of the sources, (z_1, z_2, z_3) and the body coordinates $(\bar{r}_1, \bar{r}_2, \bar{r}_3, \bar{r}_{12}, \bar{r}_{23})$. The first subscript on \bar{r}^0 refers to the source location, while the second indicates the body coordinate. The above relationships can be readily put into matrix form:

$$\begin{pmatrix} \bar{r}_{11}^0 & \bar{r}_{21}^0 & \bar{r}_{31}^0 \\ (1-\bar{r}_{12}^0) & \bar{r}_{22}^0 & \bar{r}_{32}^0 \\ (1-\bar{r}_{13}^0) & (1-\bar{r}_{23}^0) & \bar{r}_{33}^0 \end{pmatrix} \begin{pmatrix} S_1 \\ S_2 \\ S_3 \end{pmatrix} = 1/2 \begin{pmatrix} \bar{r}_1^0 \\ \bar{r}_2^0 \\ \bar{r}_3^0 \end{pmatrix}$$

Several observations can be made on the above matrix, which permit one to write the matrix corresponding to any number of the required body coordinates in closed mechanical fashion. First, the values on the diagonal of the matrix must be equal to $(1/2)$. Second, to the right of the diagonal are the sources and sinks downstream of the body points considered. Third, to the left of the diagonal are the sources and sinks upstream of the body points considered.

being established, is used for generating the values of $(\beta_x^0)_s$, and is in a position to determine the complete body form, and also the velocities anywhere in the surrounding flow field.

The axial velocity component can be found conveniently by letting,

$$(\beta_x^0)_t = \frac{(f_{x0})_t}{2} = 1 + \sum_{n=1}^{\infty} \frac{a^{-j_n \ln \frac{r}{a}}}{j_n^2(j_n)} J_0(j_n r) \quad (29)$$

The axial velocity at any point is then,

$$(\beta_x^0)_t = 1 + \sum_{n=1}^{\infty} S_n (\beta_x^0)_s \quad (30)$$

where the sign is (+) for $z > 0$, and (-) for $z < 0$.

At $z = 0$, $\beta_x^0 = 0$.

Solving Eq. 30 for $(\beta_x^0)_s = 0$ when $r = 0$, yields the location of the stagnation point.

The radial velocity component can be determined similarly, by letting,

$$(\beta_r^0)_s = \sum_{n=1}^{\infty} \frac{a^{-j_n \ln \frac{r}{a}}}{j_n^2(j_n)} J_1(j_n r) \quad (31)$$

thus, the radial velocity at any point is,

$$(\beta_r^0)_t = \sum_{n=1}^{\infty} S_n (\beta_r^0)_s \quad (32)$$

It may be desired to specify the total strength of the sources and sinks as an initial condition. This can be done conveniently by specifying the radius of the body at $z = 4cm$. Then by continuity,

$$1 - \sum_{n=1}^{\infty} S_n = (1 + \sum_{n=1}^{\infty} S_n)(1 - \frac{r^2}{r_0^2})$$

so that

$$\sum_{n=1}^{\infty} S_n = \frac{r_0^2}{r_0^2 - r^2}$$

The examples were carried out on bodies with seven coordinate points and the total source-sink strength specified. The details are presented in Appendix II, and the results in Fig. 9(a) and (b).

2. General Distributions of Source and Sink Dipoles

Clearly, one could obtain generalised body shapes using many types of source and sink distributions. However, the utilisation of source and sink distributions appears to offer an advantage in that the series expansions converge more rapidly than for the case of point sources and sinks.

The use of this method is similar to the case where sources and sinks were used.

C. Prescribed Body Coordinates and Velocity Distribution

Velocity Distribution of Sources and Sinks

The combined problem of specifying certain points on a body and certain flow conditions, and then solving for the complete body shape is often of interest. The technique for solving this problem is similar to that employed when prescribing the body shape alone.

A source or sink must be included for each point or flow condition specified. The appropriate equation relating these conditions is either 26, 30 or 32. Finally, one has a set of (s) linear equations in (s) unknowns to be solved. Upon their solution, the complete body shape can be determined using the methods described in the previous sections. An example is carried out in Appendix III. The results are shown in Fig. 10.

D. Influence of Local Curvature

Often in the design of ducted bodies, a question arises as to the influence of local body curvature on the adjacent velocity distribution. Two methods of varying the local body curvature were studied.

The first method studied, involved the calculation of bodies using eight specified body coordinates and point sources and sinks on the same. By maintaining seven of the body points the same but varying others slightly, similar bodies with different (localised) curvatures were obtained. The results of this approach are shown in Fig. 9(c). The velocities were calculated at $\alpha = 0$, and $\alpha = \pm 4^\circ$. The results are compared in Fig. 9(d). It can be seen that while the curvature effects were strong on the axial and radial components near the body, the effect on the magnitude of the resultant (meridional)

velocity was found. The streamlines behind and about the body were found to apparently change from curve. The effect of the surface curvature became negligible at approximately half the distance from the body to the duct wall.

A second method tested, was the use of a ring source in combination with a point source. The ring and point source were placed in the same plane, with the radius of the ring being close to that desired for the body. While it would have been more desirable to superimpose a ring doublet on a point source, so that there would be no change in the mass flow, the computation of the ring doublet is somewhat cumbersome due to the slow rate of convergence. Using a ring and point source, one can prescribe the closeness of the ring to the body surface arbitrarily. This follows from the boundary conditions and continuity. Since it is known that in the plane of a point and ring source, there is no axial velocity component due to the source flow, the axial velocity in this plane is wholly that of the unperturbed uniform flow. By con inuity, the radius of the body in the plane of the sources is,

$$r_c^2 = \frac{2}{\pi} (\alpha_p + \alpha_r)$$

where (α_p) and (α_r) are the strengths of the point and ring-sources respectively. Consequently, when the total source strengths are specified, the body radius is known in the plane of the sources and the radius of the ring can be placed as close to the body surface as desired.

Initial studies were made on two examples using the above method. The initial calculation assumed a value of $\alpha_r = .05 \alpha_p$, which turned out to be too small a value for the ring source, as a negligible effect was had on the body shape. When the strength of the ring source was increased to $\alpha_r = .10 \alpha_p$, significant changes in body contour occurred. The effect of this change in body contour on the velocity distribution along the duct wall was calculated, and the results are shown in Fig. 11.

COMPUTING PROCEDURE

While the primary emphasis has been placed on developing the velocity potential and stream function for various sources and sink distributions inside ducts and associated methods for determining special body contours, considerable insight into the general nature of the flow about axially symmetric curved bodies has been obtained by the obvious from the nature of the solutions, however, that a computer program can be developed as a routine for FRAY ORWELL FLOW STABILITY.

The development of the velocity potential for a point source indicates that at $r = \infty$, there is a source face velocity equal to $(\pi/2)U$. Thus the undisturbed velocity is not equal to the upstream uniform velocity as in the case of a point source if $R = \infty$ (zero free stream flow), but rather ($U - \infty$) for upstream and ($U + \infty$) for downstream.

An interesting finding, useful for comparing ducted and non-ducted flows, is that the body radius in the plane of the source (dealing here with bodies due to a single point source) is the same; i.e., $R_0 = 2a/U$ in both cases. For the body radius at $r = \infty$, however, the non-ducted case has $R_\infty^2 = 4a/U$, as compared with the ducted case

$$\frac{R_\infty^2}{R_0^2} = \frac{4a/U}{1 + 2a/U}$$

One-dimensional point: the location of the stagnation point, will be compared for the two cases. In the case of the non-ducted body (for a single point source), it occurs at $z = -(a/U)^{1/2}$; whereas in the ducted case, it may be located by writing Eq. 22 in the form, $2a/U = 1/\zeta_0^2$. Using Table II, for $r = 0$, one obtains the following comparison:

Stagnation point ducted body	Stagnation point non-ducted body	a/U
-0.10	-0.110	0.0120
-0.20	-0.224	0.0240
-0.30	-0.335	0.0367
-0.40	-0.432	0.0485
-0.50	-0.520	0.0593
-0.60	-0.597	0.0700
-0.70	-0.655	0.0800
-0.80	-0.702	0.0893
-0.90	-0.742	0.0985
-1.00	-0.761	0.1060

In conclusion, it is seen that non-ducted and ducted point source bodies are essentially the same for values of (a/U) of about 0.1 or smaller. The corresponding results for a doublet, indicate that the body shape is not appreciably affected from a doublet which is removed from (a/U) .

Finally, it is noted that the method of differentiation of the functions, it is apparent that differentiation with respect to either ζ or ζ^{-1} reduces the rate of convergence and hence increases the number of computations required to obtain an accurate solution. A

the series. Consequently, the use of doublets (ring and disk inclined) for the many or flow about bodies is particularly efficient. This amounts to an exact representation for velocity potential of a doublet is actually the result of differentiation of the corresponding velocity potential for a source. Thus, the series for the evaluation of the velocity components about a body due to a doublet in a uniform flow is difficult to compute. For the reasons indicated above, the study of doublet forms was incomplete.

For the ring doublet investigated (no. Fig. 7), the shape of the inner and outer surfaces is quite different due to the nature of the ring doublet flow. It is likely that this shape difference will diminish if the strength of the ring doublet were decreased. Thus, it appears that the use of ring doublets, sources and sinks may be a practical way of studying the flow about ring type flame holders. Of course high speed computing devices would be required to conduct a detailed study on this problem.

The investigation of the disk doublet in a uniform flow was aided by the fact that the expressions for the velocity potential for a disk doublet converges better than the velocity potential of the other doublet forms studied. For the cases which were calculated, it appears that the resultant body, (when the disk doublet is placed in a uniform flow) is very nearly a circle for body diameters up to one-half the duct diameter. For larger bodies, the shape becomes progressively blunter.

The computation of bodies of arbitrary shape is considerably reduced once the stream function and velocity components for a point source have been evaluated from tabulations. Tables I, II and III contain a sufficient range of these quantities to determine the complete flow field about a wide variety of body shapes. For rapid and approximate studies, graphical methods may be used. For detailed and precise studies, the computation can be set up on an automatic computer in a number of ways.

The influence of local body curvature is of practical interest in the design of the hub of a turbomachine. The shape of the hub influences the blade loading, at least near the hub. An important design problem is how far away, upstream from the hub, can the blade loading be affected by introducing changes in local curvature of the hub. Another problem is that of obtaining a particular velocity distribution at inlet to the machine which might be more desirable. However, when pressure causes a change in curvature, unless the change of the hub influences the velocity distribution. The results shown in Figs. 1 and 2 indicate, in a preliminary manner, that large changes in hub contour are ineffectual in bringing about significant changes in the velocity distribution.

in which there is significant change in velocity distributions, it was calculated for a transverse velocity distribution. Several points were classified as body coordinates above, so that the basic form of the b.c.b would not be completely different. The result, shown in Fig. 10, indicates, in a preliminary way at least, that the method of prescribing the velocity distribution leads to large fluctuations in b.c.b. Further, we conclude that the type of velocity distributions obtained in Fig. 9(b) are most likely to occur with practical body shapes.

TABLE I

Stress Function Γ' for a Point Source

Z	$r = 0.10$	$r = 0.16$	$r = 0.20$	$r = 0.24$
0.10	1.4626312-1	2.9364612-1	2.964575-1	3.061671-1
0.20	5.3774535-2	1.6117535-2	1.6775616-2	1.7336678-2
0.30	2.5696692-2	6.3892902-2	6.9662131-2	1.142458-1
0.40	1.6469951-2	3.9702112-2	5.9668131-2	8.0167258-2
0.50	1.1526615-2	2.8697872-2	4.3312837-2	6.0142130-2
0.60	9.0023158-3	2.2505394-2	3.4493682-2	4.8517014-2
0.70	7.519402-3	1.9949449-2	2.9254934-2	4.1484053-2
0.80	6.5204461-3	1.6716465-2	2.6921529-2	3.7093774-2
0.90	6.0264469-3	1.5000000-2	2.3665390-2	3.0451632-2
1.00	5.7053940-3	1.4533364-2	2.1941970-2	3.0373374-2
Z	$r = 0.30$	$r = 0.34$	$r = 0.38$	$r = 0.40$
0.10	3.0555570-1	3.5331537-1	3.7309714-1	3.7577306-1
0.20	2.2987228-1	2.5590553-1	2.7869358-1	2.8939878-1
0.30	1.5713956-1	1.8986709-1	2.0749902-1	2.1924607-1
0.40	1.1400474-1	1.3709725-1	1.6018088-1	1.7164549-1
0.50	8.5373626-2	1.0662204-1	1.2963489-1	1.401517-1
0.60	7.2610667-2	9.0003593-2	1.0997489-1	1.1942284-1
0.70	6.3114830-2	7.9455812-2	9.7238428-2	1.0658954-1
0.80	5.6942617-2	7.2182445-2	8.896674-2	9.7796102-2
0.90	5.2944572-2	6.7406589-2	8.3407250-2	9.1963994-2
1.00	5.0320054-2	6.4251570-2	7.9769296-2	8.8971499-2
Z	$r = 0.44$	$r = 0.48$	$r = 0.50$	$r = 0.52$
0.10	3.9746657-1	4.0763998-1	4.1236078-1	4.1609812-1
0.20	2.0694443-1	3.2668132-1	3.3498703-1	3.4294777-1
0.30	2.4176673-1	2.6308776-1	2.7334220-1	2.8335241-1
0.40	1.9433966-1	2.1445536-1	2.2765548-1	2.3554350-1
0.50	1.6209974-1	1.8115171-1	1.9526421-1	2.0642350-1
0.60	1.4053556-1	1.6140512-1	1.7884504-1	1.9355008-1
0.70	1.2616788-1	1.4661817-1	1.5752140-1	1.6866986-1
0.80	1.1457398-1	1.3661887-1	1.4708504-1	1.5764395-1
0.90	1.1015175-1	1.2972504-1	1.4001546-1	1.5046439-1
1.00	1.0583591-1	1.2506070-1	1.3520941-1	1.4571025-1
Z	$r = 0.54$	$r = 0.56$	$r = 0.58$	$r = 0.60$
0.10	4.2215459-1	4.2530698-1	4.3645154-1	4.3915588-1
0.20	3.5366592-1	3.5810601-1	3.6571167-1	3.7223714-1
0.30	2.9913934-1	3.0272182-1	3.1215262-1	3.2127746-1
0.40	2.4693521-1	2.6013520-1	2.7205577-1	2.8214057-1
0.50	2.1763734-1	2.2287777-1	2.4017212-1	2.5245097-1
0.60	1.9561015-1	2.06611485-1	2.1264505-1	2.2794115-1
0.70	1.7940810-1	1.9102517-1	2.0264798-1	2.1443789-1
0.80	1.6320970-1	1.8025504-1	1.9186916-1	2.0375540-1
0.90	1.6157679-1	1.7203854-1	1.8441590-1	1.9639574-1
1.00	1.5655968-1	1.6775420-1	1.7929138-1	1.9124347-1

TABLE I - continued

β	$r = 0.04$	$r = 0.08$	$r = 0.64$	$r = 0.68$
0.10	4.3693399-1	4.4402595-1	4.4440849-1	4.4742845-1
0.20	3.7937846-1	3.6566772-1	3.7232632-1	3.9867452-1
0.30	3.3048230-1	3.3747230-1	3.4235709-1	3.5715739-1
0.40	2.9196137-1	3.0247332-1	3.1235589-1	3.4341715-1
0.50	2.6269622-1	2.7433635-1	2.8383606-1	2.9740266-1
0.60	2.4165904-1	2.5365943-1	2.6577666-1	2.7004044-1
0.70	2.2465546-1	2.3661865-1	2.5129729-1	2.6393445-1
0.80	2.1591186-1	2.2839569-1	2.4102653-1	2.5398721-1
0.90	2.0630358-1	2.2101385-1	2.3382809-1	2.4694875-1
1.00	2.0330353-1	2.1593474-1	2.2802152-1	2.4204249-1
 Z	 $r = 0.70$	 $r = 0.72$	 $r = 0.74$	 $r = 0.76$
0.10	4.5076593-1	4.5406704-1	4.5735066-1	4.6061964-1
0.20	4.0593251-1	4.1151529-1	4.1776266-1	4.239216-1
0.30	3.6500734-1	3.7356937-1	3.8321760-1	3.9185048-1
0.40	3.3307725-1	3.4435700-1	3.5443969-1	3.6366998-1
0.50	3.0764290-1	3.2076666-1	3.3258874-1	3.4445017-1
0.60	2.9045483-1	3.0394191-1	3.1575650-1	3.2865625-1
0.70	2.7490455-1	2.9003339-1	3.0338395-1	3.1696017-1
0.80	2.6172139-1	2.7802730-1	2.9347173-1	3.0650958-1
0.90	2.6037526-1	2.7614811-1	2.8816821-1	3.0249710-1
1.00	2.5559751-1	2.6948667-1	2.8371045-1	2.9826977-1
 Z	 $r = 0.78$	 $r = 0.80$	 $r = 0.82$	 $r = 0.84$
0.10	4.6387437-1	4.6703973-1	4.7030251-1	4.7343576-1
0.20	4.3000239-1	4.3537727-1	4.4206696-1	4.4860746-1
0.30	4.0048439-1	4.0913738-1	4.1762228-1	4.2655458-1
0.40	3.7944993-1	3.8639600-1	3.9732296-1	4.0614294-1
0.50	3.5633403-1	3.6869201-1	3.8096457-1	3.9342715-1
0.60	3.4173197-1	3.5499149-1	3.644428-1	3.8209457-1
0.70	3.3076794-1	3.44101210-1	3.5979937-1	3.7363682-1
0.80	3.22882216-1	3.3711528-1	3.5229267-1	3.6765752-1
0.90	3.1715636-1	3.3213004-1	3.4741971-1	3.6302943-1
1.00	3.1314599-1	3.2801004-1	3.4277597-1	3.5920109-1
 Z	 $r = 0.86$	 $r = 0.88$	 $r = 0.90$	 $r = 0.92$
0.10	4.7666446-1	4.7863916-1	4.8209011-1	4.8637197-1
0.20	4.5178216-1	4.5697592-1	4.6726696-1	4.7362213-1
0.30	4.3534839-1	4.4422044-1	4.5318490-1	4.6225913-1
0.40	4.1907303-1	4.3012638-1	4.4132439-1	4.5267736-1
0.50	4.0603168-1	4.181116-1	4.3178105-1	4.4695453-1
0.60	3.9376777-1	4.0680700-1	4.2385700-1	4.4077600-1
0.70	3.8282252-1	3.9713412-1	4.183129-1	4.3445390-1
0.80	3.7229218-1	3.8646464-1	4.1175571-1	4.3111227-1
0.90	3.6277407-1	3.7656161-1	4.0477572-1	4.2705099-1
1.00	3.7615672-1	3.9277210-1	4.0973306-1	4.2705099-1

TABLE IX

Axial Velocity v_x^* For A Point Source

τ	$r = 0.00$	$r = 0.10$	$r = 0.20$	$r = 0.30$
0.10	4.0261733942	1.95503494-1	1.00000000	1.00000000
0.20	1.251557571	7.1457787	4.00000000	2.00000000
0.30	1.70699349	4.97501400	3.4967645	2.00000000
0.40	1.64914388	3.14666660	2.5467200	1.00000000
0.50	1.57522110	2.2461000	1.9997777	1.00000000
0.60	1.50851170	1.67734540	1.4993740	1.00000000
0.70	1.43843304	1.4094000	1.1205783	1.00000000
0.80	1.3632757	1.3166193	1.00000000	1.00000000
0.90	1.28177256	1.2079499	1.00000000	1.00000000
1.00	1.1942204	1.1360036	1.00000000	1.00000000
<hr/>				
τ	$r = 0.40$	$r = 0.50$	$r = 0.60$	$r = 0.70$
0.10	1.00000000	7.05503494-2	4.00000000	2.00000000
0.20	1.00000000	1.00000000	1.00000000	1.00000000
0.30	1.70222193	1.04473914	1.3402296	1.00000000
0.40	1.60363553	1.1205783	1.3506666	1.00000000
0.50	1.46318403	1.2079499	1.37547700	1.00000000
0.60	1.3632757	1.1360036	1.3993740	1.00000000
0.70	1.28177256	1.00000000	1.4145476	1.00000000
0.80	1.1942204	1.00000000	1.4179200	1.00000000
0.90	1.1119446	1.00000000	1.00000000	1.00000000
1.00	1.0765608	1.00000000	1.00000000	1.00000000
<hr/>				
τ	$r = 0.80$	$r = 0.90$	$r = 0.95$	$r = 1.00$
0.10	5.66387000	5.1880439-3	4.00000000	4.00000000
0.20	1.00000000	8.00000000	8.00000000	8.00000000
0.30	1.00000000	1.00000000	1.00000000	1.00000000
0.40	1.2126146	2.0121000	1.00000000	1.00000000
0.50	1.1956611	1.1156332	1.1171336	1.00000000
0.60	1.1615593	1.1313557	1.1025330	1.00000000
0.70	1.1226476	1.1021773	1.00021160	1.00000000
0.80	1.0695479	1.0757821	1.0002709	1.00000000
0.90	1.0636765	1.0546200	1.0455503	1.00000000
1.00	1.0419001	1.0366015	1.00000000	1.00000000
<hr/>				
τ	$r = 0.50$	$r = 0.60$	$r = 0.70$	$r = 0.80$
0.10	1.00000000	1.00000000	1.00000000	1.00000000
0.20	1.00000000	1.00000000	1.00000000	1.00000000
0.30	1.00000000	1.00000000	1.00000000	1.00000000
0.40	1.00000000	1.00000000	1.00000000	1.00000000
0.50	1.00000000	1.00000000	1.00000000	1.00000000
0.60	1.00000000	1.00000000	1.00000000	1.00000000
0.70	1.00000000	1.00000000	1.00000000	1.00000000
0.80	1.00000000	1.00000000	1.00000000	1.00000000
0.90	1.00000000	1.00000000	1.00000000	1.00000000
1.00	1.00000000	1.00000000	1.00000000	1.00000000

TABLE II - continued

β	$\tau = 0.25$	$\tau = 0.75$	$\tau = 0.85$	$\tau = 0.95$
0.30	1.7681072-1	1.7680948-1	1.7680945-1	1.7680943-1
0.35	1.6114992-1	1.6114990-1	1.6114988-1	1.6114986-1
0.40	1.4662062-1	1.4662060-1	1.4662058-1	1.4662056-1
0.45	1.3310137-1	1.3310135-1	1.3310133-1	1.3310131-1
0.50	1.2071167-1	1.2071165-1	1.2071163-1	1.2071161-1
0.55	1.0934206-1	1.0934204-1	1.0934202-1	1.0934200-1
0.60	9.9101179-1	9.9101177-1	9.9101175-1	9.9101173-1
0.65	9.6671167-1	9.6671165-1	9.6671163-1	9.6671161-1
0.70	9.3112097-1	9.3112095-1	9.3112093-1	9.3112091-1
0.75	8.8943003-1	8.8943001-1	8.8943000-1	8.8943000-1
0.80	8.3943000-1	8.3943000-1	8.3943000-1	8.3943000-1
0.85	7.8143000-1	7.8143000-1	7.8143000-1	7.8143000-1
0.90	7.1603000-1	7.1603000-1	7.1603000-1	7.1603000-1
0.95	6.4343000-1	6.4343000-1	6.4343000-1	6.4343000-1
1.00	5.6343000-1	5.6343000-1	5.6343000-1	5.6343000-1
β	$\tau = 1.00$			
0.30	1.7681072-1			
0.35	1.6114992-1			
0.40	1.4662062-1			
0.45	1.3310137-1			
0.50	1.2071167-1			
0.55	1.0934206-1			
0.60	9.9101179-1			
0.65	9.6671167-1			
0.70	9.3112097-1			
0.75	8.8943003-1			
0.80	8.3943000-1			
0.85	7.8143000-1			
0.90	7.1603000-1			
0.95	6.4343000-1			
1.00	5.6343000-1			

TABLE III

Radial Velocity of the A Point Source

ξ	$r = 0.10$	$r = 0.20$	$r = 0.30$	$r = 0.40$
0.10	1.5753417+1	1.2044187	1.1900777	1.1449573
0.20	1.0435389	1.0292149	1.0222692	2.4709645
0.30	1.3257056	1.0582461	1.0511751	1.4469516
0.40	1.7862543	1.0660560	1.0725574	9.5037603-1
0.50	3.4274022	5.7366084-3	6.5616260	6.2706175-1
0.60	2.9136702-1	3.9359878-2	4.041157	4.0721706-1
0.70	1.1321095-1	2.0272494-2	2.3186998	2.6661486-1
0.80	6.9620442-2	1.2712896-1	1.4738820	1.7758893-1
0.90	4.4519668-2	8.1654425-2	1.0477791	1.1177540-1
1.00	2.4777727-2	5.3300078-2	7.0637797	7.9119283-2
ξ	$r = 0.44$	$r = 0.50$	$r = 0.58$	$r = 0.64$
0.10	2.2211176	1.4772480	1.5904493	1.3996495
0.20	1.777500	1.3567358	1.2922388	1.1939577
0.30	1.2676580	1.0676456	9.9966679-1	9.4999336-1
0.40	8.8670940-1	7.4668682-1	7.3039389-1	6.9142081-1
0.50	5.9594394-1	5.3733372-1	5.1570744-1	4.9542238-1
0.60	3.9736205-1	3.4895782-1	3.57300374-1	3.4478336-1
0.70	2.6448679-1	2.5199999-1	2.4513474-1	2.5811485-1
0.80	1.7707252-1	1.7778289-1	1.6738156-1	1.6342392-1
0.90	1.1880077-1	1.1593004-1	1.1105272-1	1.1175406-1
1.00	7.9779920-2	7.5715067-2	7.7655287-2	7.6298120-2
ξ	$r = 0.56$	$r = 0.58$	$r = 0.60$	$r = 0.62$
0.10	1.5753417	1.2044187	1.1900777	1.1449573
0.20	1.0435389	1.0292149	1.0222692	1.0200773
0.30	1.3257056	1.0582461	1.0511751	1.0433307-1
0.40	1.7862543	1.0660560	1.0725574	1.0611924-1
0.50	3.4274022	5.7366084-3	6.5616260	6.0061087-2
0.60	2.9136702-1	3.9359878-2	4.041157	4.0247091-2
0.70	1.1321095-1	2.0272494-2	2.3186998	2.0801561-1
0.80	6.9620442-2	1.2712896-1	1.4738820	1.5298188-1
0.90	4.4519668-2	8.1654425-2	1.0477791	1.0661675-2
1.00	2.4777727-2	5.3300078-2	7.0637797	7.8193549-2
ξ	$r = 0.64$	$r = 0.66$	$r = 0.68$	$r = 0.70$
0.10	9.0607356-1	8.2667940-1	7.5219589-1	6.8268209-1
0.20	7.9505739-1	7.2995428-1	6.6866952-1	6.1094466-1
0.30	6.5136722-1	6.0086891-1	5.5583132-1	5.1073617-1
0.40	5.0993749-1	4.7132125-1	4.3781518-1	4.0846344-1
0.50	3.7724222-1	3.5778243-1	3.3046361-1	3.0742354-1
0.60	2.7732951-1	2.5792942-1	2.4239777-1	2.2641155-1
0.70	1.9332224-1	1.8420252-1	1.7395074-1	1.6387551-1
0.80	1.3634583-1	1.2993666-1	1.2299366-1	1.1592997-1
0.90	9.4527798-2	9.0571300-2	8.6057155-2	8.1326693-2
1.00	6.0581639-2	6.2765372-2	5.9742366-2	5.6083977-2

TABLE III - continued

	$r = 0.72$	$r = 0.74$	$r = 0.76$	$r = 0.78$
0.10	6.1284812-1	5.5299414-1	5.0527777-1	4.5353166-1
0.20	3.3639590-1	5.0471623-1	4.5374499-1	4.0233404-1
0.30	4.6785277-1	4.4291400-1	3.06668671-1	3.4755676-1
0.40	3.7877741-1	3.4117664-1	3.0000000-1	2.6217820-1
0.50	2.8459773-1	2.6304336-1	2.3774066-1	2.1785773-1
0.60	2.1068300-1	1.9496801-1	1.7746280-1	1.6593644-1
0.70	1.5860354-1	1.4167760-1	1.3048756-1	1.1851015-1
0.80	1.0843000-1	1.0126478-1	9.4553135-2	8.5089911-2
0.90	7.6404992-1	7.1922005-2	6.4997392-2	6.0753536-2
1.00	5.3775012-1	4.9581220-2	4.6030000-2	4.3750000-2
<hr/>				
	$r = 0.80$	$r = 0.82$	$r = 0.84$	$r = 0.86$
0.10	4.0434655-1	3.5672246-1	3.1223246-1	2.6580320-1
0.20	3.6463468-1	3.2206525-1	2.8118476-1	2.4185004-1
0.30	3.1101228-1	2.7560015-1	2.4133600-1	2.0017761-1
0.40	2.5292301-1	2.2425199-1	1.9689739-1	1.7082652-1
0.50	1.966133-1	1.750125-1	1.511934-1	1.315854-1
0.60	1.4769459-1	1.321083-1	1.1665457-1	1.023544-1
0.70	1.0645224-1	9.77173-1	8.6007743-2	7.4401609-2
0.80	7.775515-2	7.0000000-2	6.214788-2	5.466574-2
0.90	5.5313584-2	4.979820-2	4.4226972-2	3.9335432-2
1.00	3.8632536-2	3.4997443-2	3.1120496-2	2.7206438-2
<hr/>				
	$r = 0.76$	$r = 0.78$	$r = 0.80$	$r = 0.82$
0.30	2.3556224-1	1.9380000-1	1.6430730-1	1.3800000-1
0.40	2.0405324-1	1.6770000-1	1.4544444-1	1.2111111-1
0.50	1.7500000-1	1.4177777-1	1.1111111-1	8.8888888-2
0.60	1.5000000-1	1.2000000-1	9.9999999-2	8.3333333-2
0.70	1.2800000-1	1.0000000-1	8.0000000-2	6.6666666-2
0.80	1.0600000-1	7.4000000-2	5.4444444-2	4.4444444-2
0.90	8.5000000-2	5.2000000-2	3.4444444-2	2.7777777-2
1.00	6.3820190-2	3.2000000-2	2.1111111-2	1.5555555-2

SOLUTION OF EQUATION 2 FOR $\Omega = j^2$

Assuming in Eq. 4, and considering the case of $\Omega = j^2$, we obtain,

$$\tilde{\rho}_{xx} + j^2 \tilde{\rho} = 0$$

$$\tilde{E}_{rr} + \frac{\tilde{\rho}_{xx}}{r} - j^2 \tilde{\Omega} = 0$$

The solutions to the above equations are well known, and can be written as,

$$\tilde{\rho} = P_1 \cos(jr) + P_2 \sin(jr)$$

$$\tilde{E} = Q_1 J_0(jr) + Q_2 K_0(jr)$$

The third solution to Eq. 4 is,

$$\tilde{\rho} = (Y_1 \cos(jr) + Y_2 \sin(jr)) (Q_1 J_0(jr) + Q_2 K_0(jr))$$

where (Y_0) is the modified Bessel function of the first kind of zero order and (K_0) is the modified Bessel function of the second kind of zero order.

It is of interest to determine whether the boundary conditions for a point source can be satisfied with the solution above. Assuming condition I, it is apparent that the above solution is periodic so that a series solution cannot represent this condition.

A series solution of theoretical interest can be found for the above solution that represents a flow within a duct of constant diameter. To satisfy the condition of zero radial velocity at the duct wall, one can write,

$$\tilde{\rho} = I_0(jr)K_1(j) - K_0(jr)I_1(j)$$

where (I_1) is the modified Bessel function of the first kind of the first order, and (K_1) is the modified Bessel function of the second kind of the first order. The form of the solution is a result of the fact that neither (I_1) or (K_1) have real roots except at $r = 0$, (Ref. 6), so that a combination of the two functions is required to obtain a function that is zero for some value of (r) , i.e., satisfies the condition of zero radial velocity at the duct wall.

A flow model, which can be satisfied by the solution obtained above, is that of a periodic distribution of sources and sinks along one duct axis. Considering that the sources and sinks are spaced (b) radii apart, and that flow symmetry exists at these points, one has,

$$\left(\frac{r}{r_0} \cos \theta\right)^n = \left[I_0(jr)K_1(j) - K_0(jr)I_1(j)\right] \cdot \left(r_0^2 \cos \theta - r^2 \sin \theta\right)$$

where $a = 1, 2, 3, 4, \dots$

Thus, $I_2 = 0$, and $j = \pm \pi/a$, so that one has,

$$S = \sum_{n=1}^{\infty} A_n \left(I_0(j_n r) K_1(j_n) - K_0(j_n r) I_1(j_n) \right) \cos j_n a \quad (I-1)$$

To determine the coefficients, (A_n) , Cauchy's theorem can be applied. With alternating sources and \sin^{2a} or \cos^{2a} strength, one can use this theorem midway between them, i.e., when

$$z = \frac{2a-1}{2} b$$

Differentiating Eq. I-1, with respect to (z) , multiplying through by

$$(r \sin j_n \frac{2a-1}{2} b)$$

and integrating the result at

$$z = \frac{2a-1}{2} b$$

yields for the left hand side,

$$\frac{1}{2\pi} \int_0^{2a} \left(A_n \right)_n \cdot \frac{2a-1}{2} \sin j_n \frac{2a-1}{2} b r dr = 0$$

The above integral is valid when (p) is odd, $(j_p = p\pi/b)$.

Thus, let $p = 2u-1$, where $u = 1, 2, 3, 4, \dots$. The (+) sign holds for odd values of (u) , the (-) sign for even values. The value of the above integral is (i_m) as the flow of each source splits, $(2\pi u)$ going in either direction.

For the right hand side (see above),

$$\begin{aligned} 0 &= -\frac{i}{\pi} \frac{1}{p} I_1(j_p) \int_0^1 r I_0(j_p r) \sin^2 j_p \frac{2a-1}{2} b r dr \\ &\quad + i_p j_p I_1(j_p) \int_0^1 r K_0(j_p r) \sin^2 j_p \frac{2a-1}{2} b r dr \end{aligned}$$

Performing the integration, noting that

$$\lim_{r \rightarrow 0} r j_p K_1(j_p r) = 1$$

yields,

$$n = \frac{A_p I_1(j_p)}{j_p}$$

The resultant expression for the velocity potential is,

$$\phi = z \sum_{n=1}^{\infty} I_n \left[I_0(j_n r) \frac{I_1(j_n)}{I_1(j_0)} - I_0(j_n r) I_1(j_n) \right] \cos j_n z$$

where $j_n = (2n-1) \pi / b$.

APPENDIX II

Calculation of Special Body Curves

Table 4

The body coordinates and source locations shown are:

	s	t		s	t
s_1	-0.59	.36	s_5	-0.165	.45
s_2	-0.49	.40	s_6	0	.70
s_3	-0.365	.50	s_7	.19	.15
s_4	-0.26	.60	s_8	.62	-

Instead of specifying eight body coordinates, seven are specified along with the condition that $s_8 = .500$. Eight linear equations in eight unknowns can now be set up. To do this requires the determination of 64 coefficients. Taking the first body coordinate, and determining the value of the stream function there using Eq. 26,

$$0 = .045 - s_1 \bar{Y}_{11}^0 - s_2 \bar{Y}_{21}^0 - s_3 \bar{Y}_{31}^0 - s_4 \bar{Y}_{41}^0 - s_5 \bar{Y}_{51}^0 - s_6 \bar{Y}_{61}^0 - s_7 \bar{Y}_{71}^0 - s_8 \bar{Y}_{81}^0$$

The balance of \bar{Y}^0 are obtainable from Table I. For

$$\bar{Y}_{21}^0, \text{ ini} = 0, \text{ so that } \bar{Y}_{11}^0 = 1/2. \text{ For } \bar{Y}_{31}^0, \text{ ini} = .10, \text{ so that } \\ \bar{Y}_{21}^0 = .3456.$$

Continuing in this manner, all the coefficients for the eight equations can be quickly found. Setting the result up in matrix form

.500	.346	.266	.177	.128	.084	.062	.048	s_1	.145
.614	.500	.425	.317	.249	.151	.110	.067	s_2	.300
.638	.555	.500	.410	.304	.242	.188	.124	s_3	.195
.663	.594	.570	.390	.336	.342	.266	.190	s_4	.100
.690	.640	.620	.554	.500	.409	.334	.237	s_5	.211
.696	.674	.655	.609	.576	.500	.413	.338	s_6	.245
.701	.690	.670	.652	.620	.575	.500	.353	s_7	.201
1	1	1	1	1	1	1	1	s_8	.500

The above matrix was solved by hand, by diagonalizing it. The results were

$$s_1 = .243 \quad s_2 = -.567 \quad s_3 = .977 \quad s_7 = -.102$$

$$s_4 = -.214 \quad s_5 = .296 \quad s_6 = -.232 \quad s_8 = .159$$

To obtain the velocities, Tables II and III can be used. At the axial velocity at $s = 0$, $r = 1$, one has by Eq. 30,

$$(A_{\infty})_{\text{axial}} = 1 + S_1(S_1^*)_1 + S_2(S_2^*)_2 + S_3(S_3^*)_3 + S_4(S_4^*)_4 + S_5(S_5^*)_5 + S_6(S_6^*)_6 \\ - S_7(S_7^*)_7 - S_8(S_8^*)_8$$

To find $(S_1^*)_1$, the values $s = .53$, $r = 1$ from Table II correspond to $(S_1^*)_1 = .780$. The values of (S_i) are known from the solution of matrix, and the remaining velocity terms can be found from the tables. The radial velocities are calculated in the same manner, using Table III.

Body II

The body coordinates and source locations chosen are:

	s	r		s	r
S_1	-.90	.10	S_3	-.35	.50
S_2	-.71	.20	S_4	-.22	.60
S_5	-.57	.30	S_6	0	.70
S_7	-.45	.40	S_8	-.20	—

The sum of the source strengths was fixed at .506. The results of the calculation are:

$$S_1 = .009$$

$$S_3 = .116$$

$$S_2 = .018$$

$$S_5 = .234$$

$$S_4 = .071$$

$$S_7 = .204$$

$$S_6 = .057$$

$$S_8 = .180$$

APPENDIX III

Calculation of Circular Body Drag Coefficient
Using Velocity Distribution

The following conditions are prescribed:

Body coordinates:

x	y
-45	-40
0	.70
.52	.80

Velocity distribution at $z = 0$:

$$(U_s)_{y=0} = 1.2(U_s)_{y=.7}$$

$$(\bar{U}_s)_{y=.7} = 1.033(\bar{U}_s)_{y=.8}$$

$$(U_s)_{y=.8} = 1.067(U_s)_{y=.7}$$

The total source strength will be .596.

There are seven conditions specified, requiring seven sources and sinks. The location of these sources and sinks are:

x	y	x	y
S_1	-4.71	S_2	-4.35
S_3	-4.57	S_4	0
S_5	-4.45	S_6	.20
S_7	-4.35		

Note that the arrangements of sources departs from the method used in Appendix II, where they were located at the same (x) coordinate as the body points.

The set up of the three equations for the body coordinates follows the same approach used in Appendix II. The equations for the velocity conditions are set up as follows:

$$S_1 = \frac{1}{2} \left(\frac{1}{\rho} \frac{\partial^2 \phi}{\partial x^2} + \frac{1}{\rho} \frac{\partial^2 \phi}{\partial y^2} + \frac{1}{\rho} \frac{\partial^2 \phi}{\partial z^2} - \frac{1}{\rho} \frac{\partial^2 \phi}{\partial t^2} \right)$$

at $t = 0$, $y = 1$, and $z = 0$, $\rho = .7$, and equating the two expressions to the propulsive ratio, and multiplying both sides by $.714 \times 10^{-3}$ accessory coefficients. This procedure is repeated three times, once for each velocity condition. Thereupon, the final system of equations may be written as,

$$\begin{pmatrix} .754 & .634 & .502 & .396 & .267 & .155 & .114 \\ .724 & .704 & .678 & .651 & .600 & .500 & .410 \\ .679 & .674 & .671 & .666 & .658 & .634 & .500 \\ .267 & .289 & .287 & .270 & .211 & 0 & -.246 \\ .192 & .215 & .224 & .216 & .169 & 0 & -.158 \\ .308 & .122 & .129 & .126 & .100 & 0 & -.093 \end{pmatrix} \begin{pmatrix} S_1 \\ S_2 \\ S_3 \\ S_4 \\ S_5 \\ S_6 \\ S_7 \end{pmatrix} = \begin{pmatrix} .000 \\ .245 \\ .320 \\ .200 \\ .153 \\ .067 \\ .506 \end{pmatrix}$$

The resultant values for the source and sink strengths are:

$$S_1 = 5.691 \quad S_3 = 5.660 \quad S_5 = 25.173 \quad S_7 = -.525$$

$$S_2 = -.497 \quad S_4 = 17.383 \quad S_6 = 8.348$$

Having found the source and sink strengths, the complete body shape can be found by utilizing Eq. 28. The results are shown in Fig. 10.

REMARKS

1. Lamb, H., "A Source In A Rotating Fluid", *The Quarterly Journal Of Mathematics And Applied Mathematics*, Vol VIII, Part 1, Cambridge University Press.
2. Lamb, H., "Hydrodynamics" Sixth Edition, 1945, Dover Publications, New York.
3. Mylie, G. R., Jr., "Advanced Engineering Mathematics", First Edition, 1951 McGraw-Hill Book Company, Inc., New York.
4. Harvard Computation Laboratory, "Design and Operation of Digital Calculating Machinery - Progress Report #41", August 1955, Cambridge, Massachusetts.
5. Watson, G. N., "Theory of Bessel Functions", Second Edition, 1945, Cambridge, At the University Press.
6. Smyth, W. R., "Static and Dynamic Electricity", First Edition, 1930, McGraw-Hill Book Company, Inc., New York.
7. Macmillan, N.J., "Bessel Functions For Engineers", First Edition, 1934, Oxford University Press, London.
8. Von Karman, T., "Calculation of Pressure Distribution On Airship Hulls", NACA TM 574, July 1930.
9. Weinstein, A., "On Axially Symmetric Flows", *Quarterly Of Applied Mathematics*, Vol V, No. 4, January 1948.
10. Brezin, J. P., "Two-dimensional Flow About Half Bodies Between Parallel Walls", *Journal of Applied Mechanics*, Vol 22, No. 1, March 1955.
11. Seidewsky, M.A., and Sternberg, E., "Elliptic Integral Representation of Axially Symmetric Flows", Research Project #955, February 1, 1949, Illinois Institute of Technology.
12. Brunauer, S. A., "Axially Symmetric Free Streamline Flow About Tandem Discs", Masters Thesis, January 1951, Illinois Institute of Technology.
13. Streeter, V.L., "The Ring Doublet In Ideal Fluid Flow", Research Project #955, June 1, 1951, Illinois Institute of Technology.
14. Kragels, F., von Brand, M., "Stream Functions and Velocity Fields of Spatial Sources-Paths and Their Utility Use for the Determination of the Angles and Positions of Diffracting Edges of Rotating Circular Bodies, with Examples", Translated from German Document, AIR Documents Division, T-2, AG, Wright Field, Microfilm No. RG-1106, P-2602.

25. Miller, A., "Some Results on Generalized Axially Symmetric Potentials", AF Contract (18-600)-573-007, October 1955.

26. Minke, G.A., "Cylindrical Harmonic Functions in Three Dimensions", Technical Report 22, June 1955, Carnegie Institute of Technology.
27. Armstrong, A.H., "Axisymmetric Cavity Flow", Armament Research Establishment, Report 12/53, June 1953
28. Armstrong, A.H., "An Extension of the Hydrodynamic Source-Sink Method for Axisymmetric Bodies", Armament Research Establishment, Report 59/54, December 1954.
29. Kaplan, C., "Is a New Method for Calculating the Potential Flow Past a Body of Revolution", NACA Report 753, 1942.
30. Milne-Thomson, L.M., "Theoretical Hydrodynamics", 1950, The Macmillan Company, New York
31. Whittaker, E.T., and Watson, G.N., "Modern Analysis", Fourth Edition, 1943, Cambridge, At the University Press, London.
32. Bateman, H., "Partial Differential Equations of Mathematical Physics", First Edition, 1934, Dover Publications, New York.
33. Gray, A., Mathews, J. R., and MacRobert, T.M., "Bessel Functions", 1922, The Macmillan Company, New York
34. Carslaw, H.S., and Jaeger, "Conduction of Heat in Solids", 1947, Oxford, at the Clarendon Press.

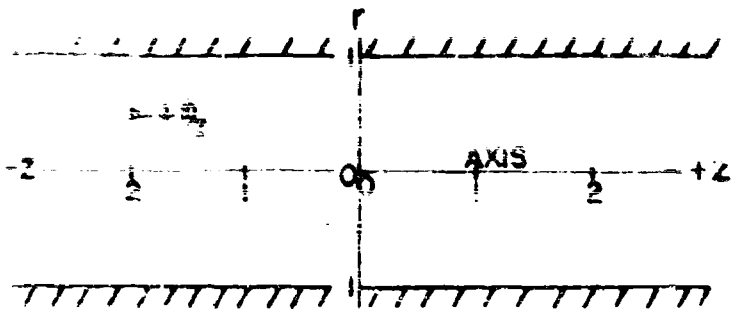


FIGURE 1. COORDINATE SYSTEM USED

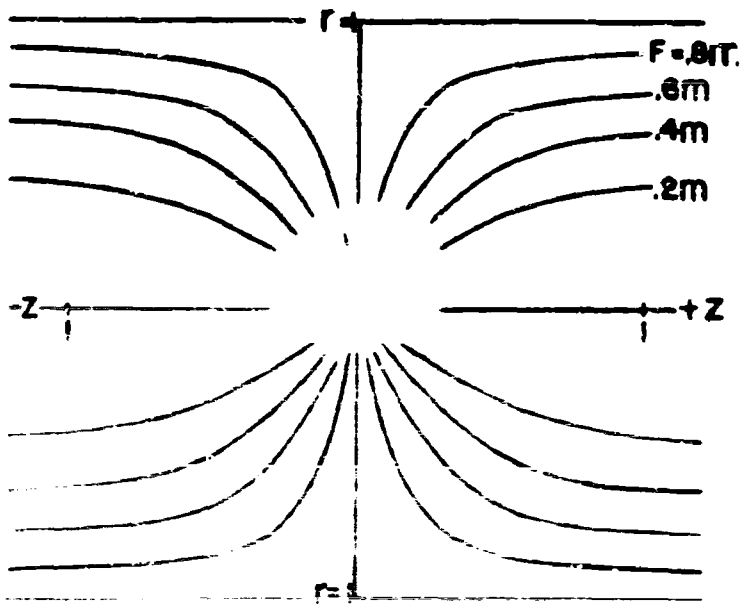


FIGURE 2. STREAMLINES OF A POINT SOURCE

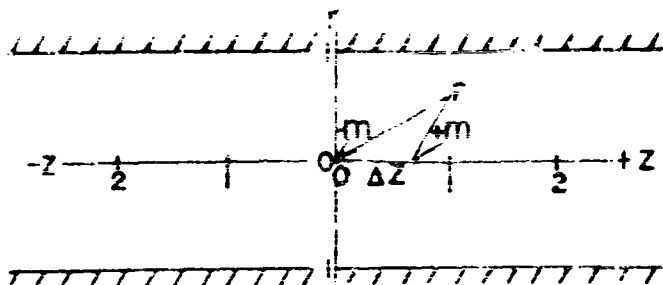


FIGURE 3. DERIVATION OF THE VELOCITY POTENTIAL
FOR A DOUBLET

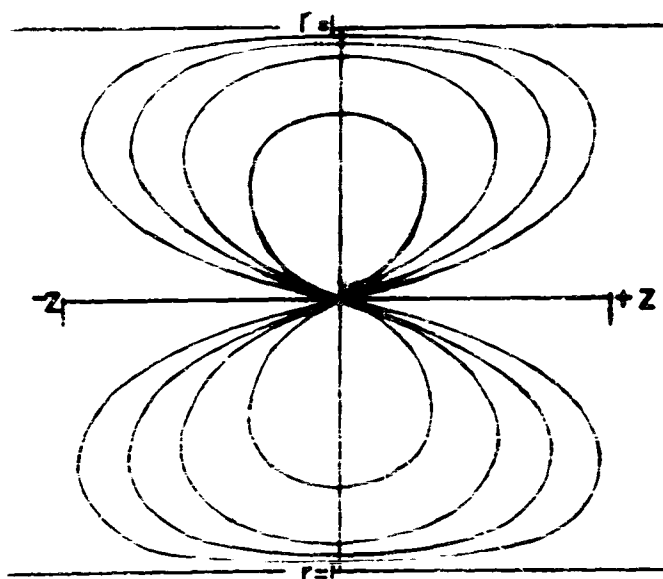


FIGURE 4. STREAMLINES OF A DOUBLET

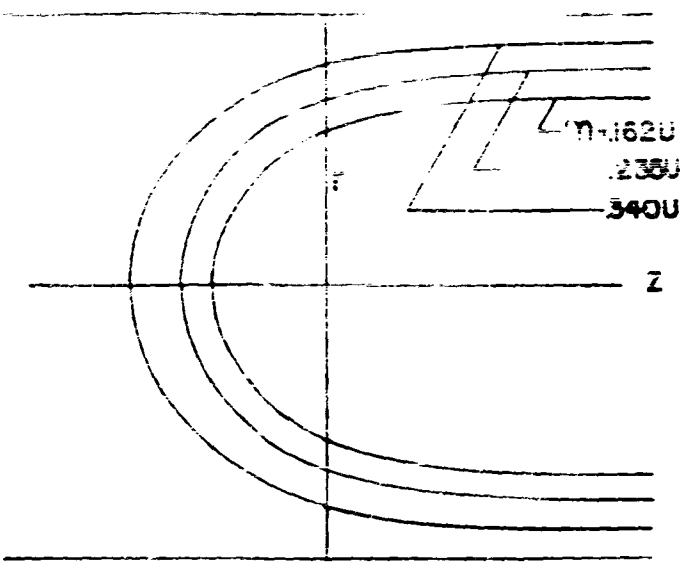


FIGURE 5. POINT SOURCES IN A UNIFORM FLOW

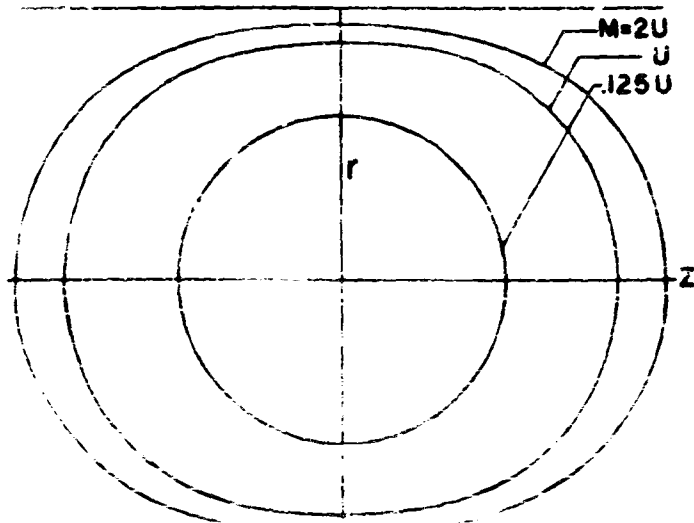


FIGURE 6. DOUBLETS IN A UNIFORM FLOW

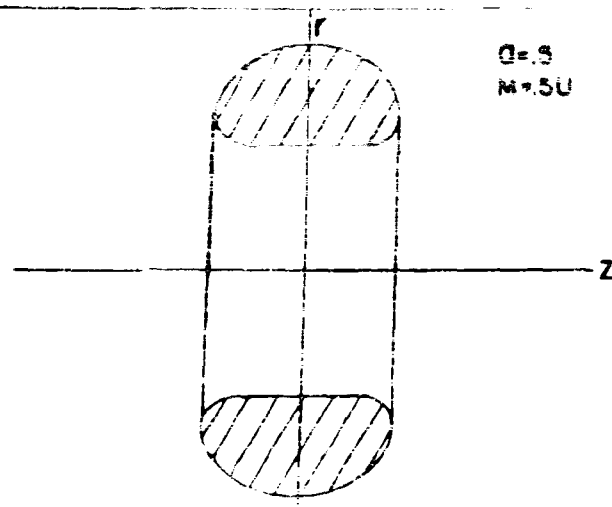


FIGURE 7 RING DOUBLET IN A UNIFORM FLOW

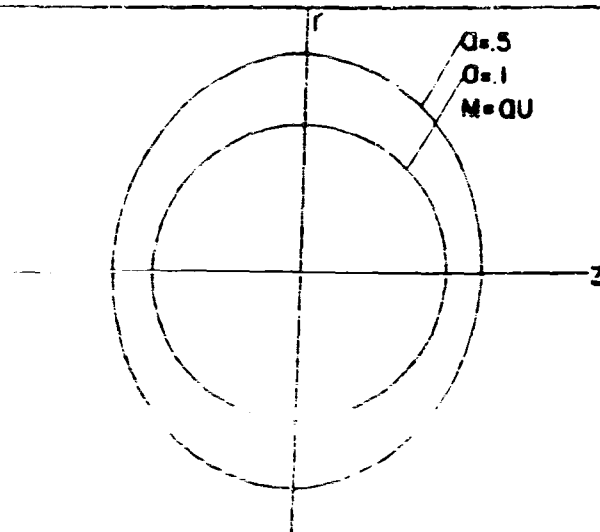
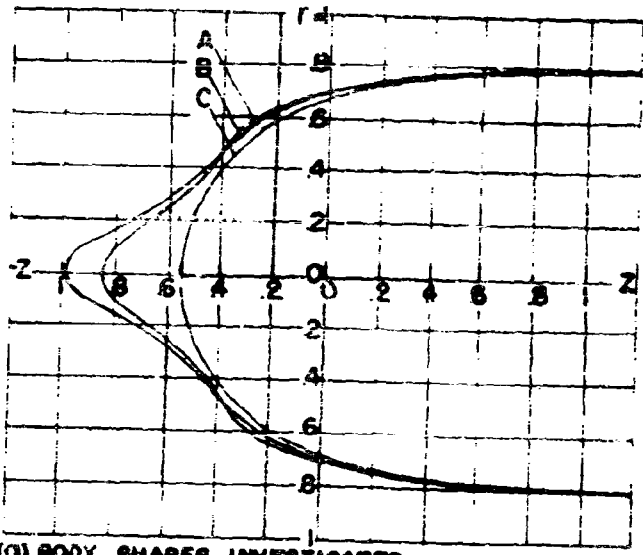
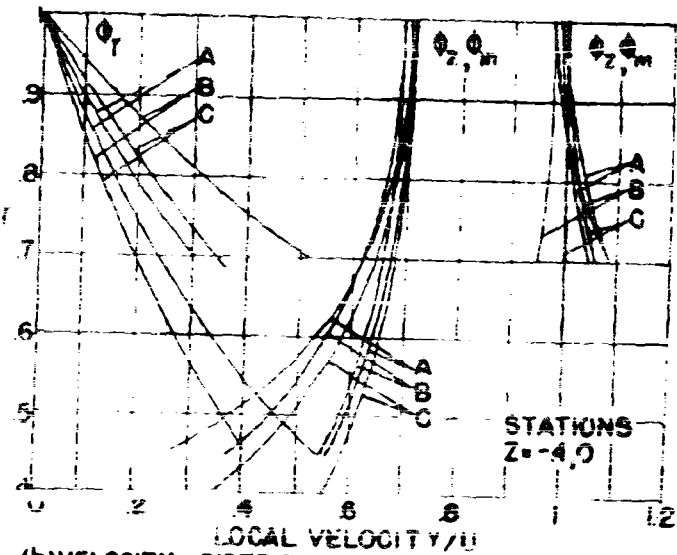


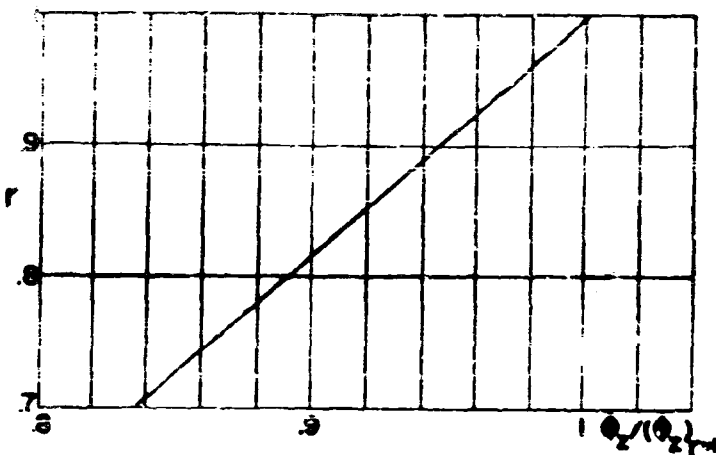
FIGURE 8 DISK DOUBLET IN A UNIFORM FLOW



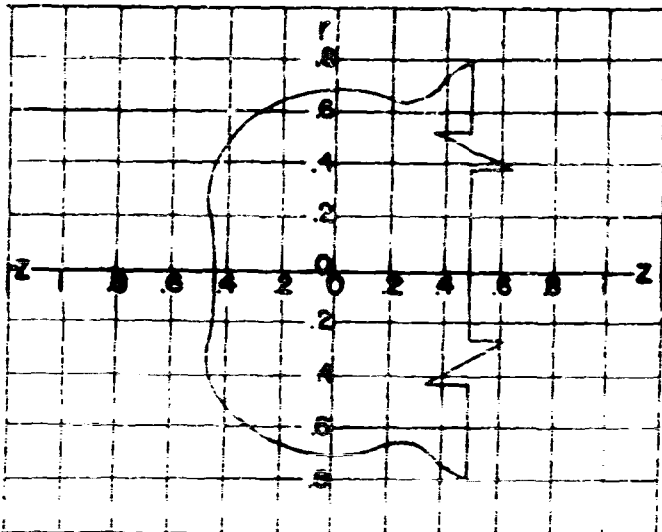
(a) BODY SHAPES INVESTIGATED



(b) VELOCITY DISTRIBUTIONS FOR BODIES (A,B,C)
FIGURE 9. ARBITRARY BODY SHAPES INVESTIGATED

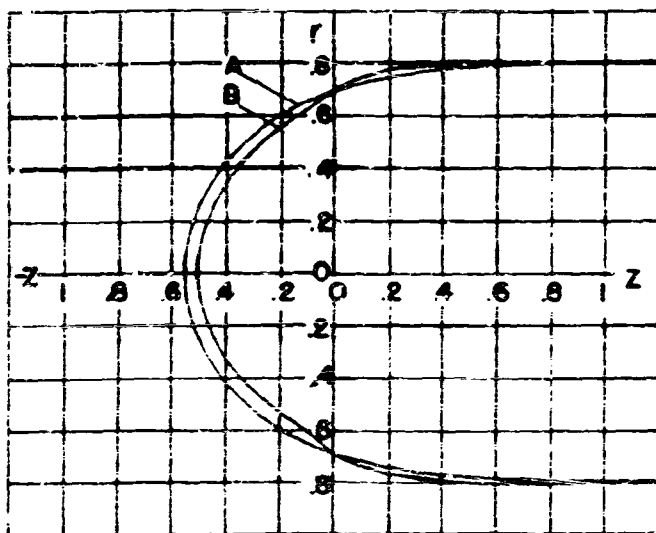


(I) PRESCRIBED VELOCITY DISTRIBUTION AT $z=0$

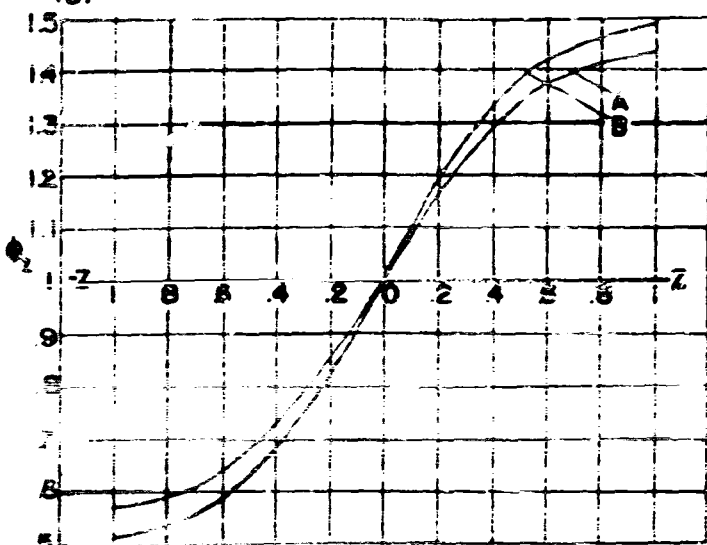


(II) RESULTANT BODY

FIGURE 10. RESULTANT BODY FOR A PRESCRIBED
VELOCITY DISTRIBUTION



(a) LOCAL EFFECT OF A RING SOURCE



(b) VELOCITIES AT THE WALL ($V = 1$)

FIGURE 11. EFFECT OF LOCAL CURVATURE

UNCLASSIFIED

**40000
40000**

Armed Services Technical Information Agency

Reproduced by

DOCUMENT SERVICE CENTER

KNGTT BUILDING, DAYTON 2, OHIO

**FOR
MICRO-CARD
CONTROL ONLY.**

110F11

NOTICE: WHEN GOVERNMENT OR OTHER DRAWINGS, SPECIFICATIONS OR OTHER DATA ARE USED FOR ANY PURPOSE OTHER THAN IN CONNECTION WITH A DEFINITELY IDENTIFIED GOVERNMENT PROCUREMENT OPERATION, THE U. S. GOVERNMENT HEREBY DISCLAIMS ALL RESPONSIBILITY, AND ANY OBLIGATION WHATSOEVER, AND THE FACT THAT THE GOVERNMENT MAY HAVE FORMULATED, FURNISHED, OR IN ANY WAY SUPPLIED THE SAID DRAWINGS, SPECIFICATIONS, OR OTHER DATA IS NOT TO BE RECKONED AS AN INDICATION OF THE QUALITY OF THE DRAWINGS, SPECIFICATIONS, OR OTHER DATA, OR AS AN ENDORSEMENT OF THE HOLDER OR ANY OTHER PERSON OR CORPORATION, OR CONVEYANCE AND ASSUMPTION OF RESPONSIBILITY FOR THE USE OR SEALESSING OF THE DRAWINGS, SPECIFICATIONS, OR OTHER DATA. IT MAY NOT BE REPRODUCED, COPIED, OR DUPLICATED, EXCEPT AS PROVIDED IN THE CONTRACT WHICH PROVIDED FOR THIS DRAWING.

UNCLASSIFIED